



UNIVERSITY
OF TRENTO

DEPARTMENT OF INFORMATION AND COMMUNICATION TECHNOLOGY

38050 Povo – Trento (Italy), Via Sommarive 14
<http://www.dit.unitn.it>

FREQUENCY DOMAIN TESTING OF WAVEFORM DIGITIZERS

Dario Petri

March 2004

Technical Report # DIT-04-046

Frequency-Domain Testing of Waveform Digitizers

Dario Petri, *Member, IEEE*

Abstract. An easy to use, robust and accurate frequency-domain procedure for estimating the spectral performance of waveform digitizers is considered in this paper. Its properties are analyzed and almost unbiased estimators are proposed along with simple but accurate expressions for their variances. Experimental results are presented to validate the proposed analysis. Directions and criteria useful for the design of the test procedure are also included.

Keywords: Analog-digital conversion, quantization, frequency domain analysis, discrete Fourier transform.

I. INTRODUCTION

Due to the high performance of available sinewave sources, modern digitizer testing procedures usually consider a spectrally pure sinewave as input signal. The data sequence provided by the digitizer under test, when fed with a full-scale input, is then processed in order to estimate the quality parameters of such a device. Obviously, the accuracy of the estimated parameters depends on the uncertainties originating both in the employed test set-up and in the numerical estimation procedure. Thus, signal processing algorithms must be carefully applied in order to ensure good estimation accuracy. This is the issue addressed in this paper.

A simple yet often sufficiently accurate model for the observed digitizer output data consists in a set of sinewave components embedded in white, or at least weakly-correlated, zero-mean noise that originates inside the digitizer itself [1], [2]. Consequently, the problem of evaluating the spectral performance of a given digitizer reduces to the estimation of each spectral line power and of the broadband noise level. Such quantities may then be employed to evaluate overall spectral figures of merits of the digitizer, such as spurious-free dynamic range (*SFDR*), signal-to-noise-and-distortion ratio (*SNDR*) or total harmonic distortion (*THD*).

The estimation of multiple sine parameters from a noisy data record is a well-known issue, which has been analyzed in detail throughout scientific literature [3], [4]. The major techniques useful for addressing such a problem can be classified in parametric and non-parametric ones.

Parametric procedures are model-based and require computationally intensive algorithms to determine the coefficients of the model that fits the available data. Signal parameters can then be estimated from such coefficients. This approach has the advantage of being very selective, that is capable of dealing with spectral lines that are closely spaced in frequency, and almost statistically efficient, that is based on estimators characterized by a variance close to the Cramer-Rao Lower Bound (*CRLB*) [5]. Unfortunately, when the analyzed signal contains many spectral lines, as often occurs in digitizer testing, the selectivity capability abruptly reduces and the determination of the model order can produce estimation blunders [3], [5]. In fact, if a slightly larger or smaller than needed set of coefficients is fitted to the data, artifacts arise that may induce in major estimation errors. This characteristic, along with the required high computational effort, can make such procedures unsuitable for many digitizer testing problems.

Opposite, the model order issue does not apply when using non-parametric techniques, which estimate the spectral parameters of interest by evaluating at first the Discrete Fourier Transform (DFT) of the digitizer output and then the rms-values of each spectral tone and of the broadband noise. Moreover, non-parametric techniques exhibit lower computational effort due to the availability of Fast Fourier Transform (FFT) algorithms. However, such advantages are achieved at the expense of decreased frequency selectivity and statistical efficiency [3]. Since the selectivity and efficiency reduction can be compensated by respectively increasing the observation interval length or the number of analyzed samples (both issues often achievable when testing a digitizer), frequency-domain based estimation methods can be widely applied for waveform digitizer testing.

In the following, capabilities and limitations of most common non-parametric techniques are briefly analyzed at first. Then, the approach proposed in [1] is revisited and the accuracy

of the estimated parameters is evaluated. The provided results are then employed to derive criteria for achieving an optimum design of the test procedure. Finally, experimental results are presented.

II. DIGITIZER OUTPUT SIGNAL MODEL

When an actual digitizer is stimulated by a pure sinewave, several kinds of disturbances other than the quantization error affect the output data:

- a *DC* offset, producing a spectral line at zero frequency;
- harmonics of the input sinewave, due to integral nonlinearities and analog circuitry nonlinear distortion;
- nonharmonic spurious tones, due to clock feedthrough, interferences, ... ;
- broadband noise, due to differential nonlinearity, clock jitter, analog circuitry noise,

Thus, a record of N samples of the digitizer output $y[\cdot]$ can be described using the model:

$$y[n] = C + x_1[n] + x_H[n] + x_S[n] + r[n] \quad n = 0, \dots, N-1 \quad (1)$$

in which C is the *DC* offset, $x_1[\cdot]$ is the tone at the input sinewave frequency, $x_H[\cdot]$ represents the harmonics of the test sinewave, $x_S[\cdot]$ models the spurious tones and $r[\cdot]$ represents any kind of broadband disturbance, including quantization error.

The parameters to be estimated for the determination of digitizer figures of merits are the power of the broadband noise σ_r^2 and the square rms values σ_i^2 , $i = 0, 1, \dots, H, \dots, H+S+1$ of the *DC* offset ($i = 0$), of the tone at the input frequency ($i = 1$), of the H harmonics ($i = 2, \dots, H+1$) and of the S spurious tones ($i = H+2, \dots, H+S+1$).

The sensitivities to broadband noise of the presented estimators are compared with the corresponding *CRLB*. Since in most practical situations the noise can be considered normally distributed [2] and the power estimators are almost unbiased, we have [5], [6]:

$$CRLB[\hat{\sigma}_i^2] = \frac{4}{N} \sigma_r^2 \sigma_i^2, \quad i = 1, \dots, H+S+1, \quad CRLB[\hat{\sigma}_r^2] \cong \frac{2}{N} \sigma_r^4. \quad (2)$$

III. DIGITIZER TESTING IN THE FREQUENCY-DOMAIN

Digitizing system testing in the frequency-domain is based on the Windowed Discrete Time Fourier Transform (WDTFT) of (1), that is the continuous-frequency transform of the weighted system output, defined as:

$$Y(\lambda) = \sum_{n=0}^{N-1} w[n] y[n] e^{-j\frac{2\pi}{N}\lambda n}, \quad \lambda \in [0, N) \quad (3)$$

where $w[\cdot]$ is the applied window sequence and λ is the normalized frequency expressed in bin. However $Y(\lambda)$ is often evaluated only for integer values of λ by applying an FFT algorithm, so that the so called Windowed Discrete Fourier Transform (WDFT) results.

As sketched in Fig.1, the magnitude of (3) exhibits a broadband term and a number of separated peaks, each one located at the normalized frequency of the corresponding spectral line and reproducing the behavior of the window spectrum mainlobe. In this figure, a linear scale is used for the frequency axis, and a logarithmic scale is adopted for the amplitude axis, while only positive frequency components have been considered due to the Hermitian symmetry of the spectrum. Notice that both $Y(0)$ and $Y(N/2)$ will be included in the calculations, in order to avoid any information loss.

Provided that the spectrum of the digitized data behaves as shown in Fig.1, simple and accurate estimators for the signal parameters can be achieved. To this aim, the frequency axis is split in the following sets, identified according to the signal components to which they refer:

- the intervals B_i associated to the i -th narrowband component, which includes N_i WDFT samples, $i = 0, \dots, H+S+1$;
- the set B_r corresponding to the broadband noise, which contains N_r WDFT samples;

Moreover, the following constraints have to be satisfied:

- (i) the bands B_i , $i = 0, \dots, H+S+1$, and the set B_r do not overlap;
- (ii) the contribution from all the tones of the digitized signal to the power inside the set B_r is enough small;
- (iii) the contribution to the power inside the band B_i from all other tones of the digitized signal is sufficiently small.

In section V it is shown how to design the test procedure in order to meet requirements (i)-(iii). Notice also that the sets depicted in Fig.1 do not necessarily cover the whole frequency axis, that is, some WDFT samples can be excluded from the estimation procedure.

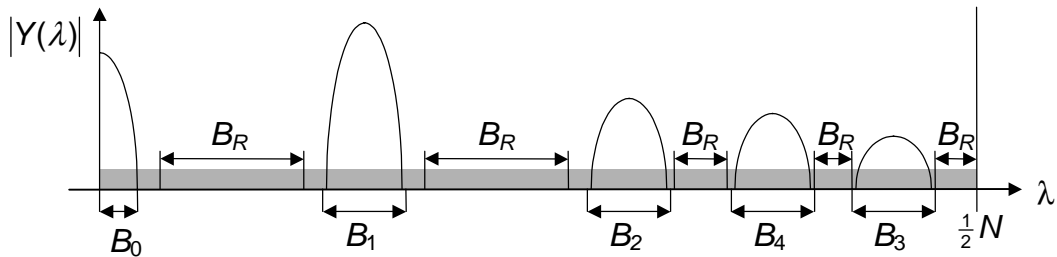


Fig. 1. Behavior of the spectrum of a digitizer output when a pure sinewave signal is employed as input stimulus ($H = 2$, $S = 1$).

IV. ANALYSIS OF FREQUENCY-DOMAIN TEST METHODS

Depending on the sampling strategy applied during digitizer data collection, various techniques for the estimation of narrowband component powers can be employed. Such techniques are analyzed in this section, along with that adopted for estimating the power of the broadband noise.

A. Estimation of Narrowband Components: Coherent Sampling

Coherent sampling occurs when the digitizer output $y[\cdot]$ is a periodic signal and the analyzed data record contains an integer number J of signal cycles, that is when:

$$JT_1 = NT_S \quad (4)$$

where $T_1 = 1/F_1$ is the signal period, while $T_S = 1/F_S$ is the sampling period. Whenever possible, J and N should be relatively prime numbers. In fact, this choice allows the maximization of the number of stimulated digitizer output codes for a given number N of collected samples [7]. However, if spurious tones are present in the digitized data, coherent sampling can not be achieved.

When (4) holds true, windowing is not required and each signal tone results in only one (unwindowed) DFT sample. In such a case, J represents the location (in bins) of the spectrum peak related to the input sinewave frequency, while iJ , $i = 2, \dots, H+1$ are the locations of harmonics (if $iJ > N/2$, the aliased lines must be considered). The following tone power estimator can be applied (Appendix A):

$$\hat{\sigma}_i^2 = \frac{2}{N^2} |Y[iJ]|^2 - \frac{2}{N} \hat{\sigma}_r^2 \quad i = 0, 1, \dots, H+1 \quad (5)$$

where $\hat{\sigma}_r^2$ represents the noise power estimator, and will be analyzed in the following. It can be shown that, as soon as the amplitude of the considered spectral line is sufficiently greater than the broadband noise level, (5) is an almost unbiased estimator and we have (Appendix B):

$$\text{var}[\hat{\sigma}_i^2] \cong \frac{4}{N} \sigma_r^2 \sigma_i^2 \quad i = 0, 1, \dots, H+1 \quad (6)$$

in which $\text{var}[\cdot]$ represents the variance of the random variable at its argument. By comparing (6) and the leftmost equation in (2) it can be concluded that maximum statistical efficiency is achieved by the DFT-based estimator when coherent sampling occurs. In fact, it can be shown that (5) coincides with the maximum likelihood estimator of the tone power [5].

B. Estimation of Narrowband Components: Noncoherent Sampling

Whenever possible, coherent sampling is the best choice for digitizer testing. However, when failing to observe an integer number of periods of even a single tone of (1), the tone energy is spread over the whole frequency axis, and the estimation of tone powers can be significantly biased by the energy leaking from neighboring tones. This occurs, for instance, when the digitized data contain spurious components or when T_1/T_S is an irrational number due to lack of synchronization between the sampling rate and the input sinewave frequency.

The effects of spectral leakage can be reduced by applying a suitable window sequence to the digitized data prior to their discrete Fourier transformation, as (3) shows.

An estimate of the rms-value of each tone can then be carried out through a peak search applied on the WDFT magnitude. However, unlike the coherent sampling case, the discrete spectrum peaks do not exactly correspond to the frequency locations of the signal tones, so that severely biased power estimators may results. The most common procedures employed to compensate for the effects of such phenomenon are:

- *zero-padding*, which allows the reduction of the frequency distance between two adjacent WDFT samples; it consists in adding zeros to the sequence of digitized data before the Fourier transformation [3];
- *Newton*-based algorithms, which allows the evaluation of the distance between a WDFT magnitude peak and the frequency of the corresponding tone [8];
- *flat-top* windows, designed in order to reduce to an acceptable value the effect of frequency granularity on the estimated tone power [9], [10];
- *interpolation*-based methods, which achieve estimate of the tone power by processing two or more samples in the neighborhood of each WDFT magnitude peak [11], [12];
- *energy*-based method, which evaluates the tone power by computing the energy falling inside a frequency band approximately covering the window spectrum mainlobe [13].

Some comments follow on the properties of the listed techniques. Zero-padding is a computationally-intensive technique since the length of the Fourier transformation must be appropriately increased. Similarly, the Newton- and interpolation-based techniques require a

relatively high computational effort and a thorough knowledge of the spectral behavior of the applied window. While easy to handle, flat-top-based algorithms lightly reduce frequency selectivity and the statistical efficiency of the estimators. Conversely, the energy-based method requires only overall window spectrum specifications and is characterized by a moderate computational burden. As shown below, it does not rely heavily on the signal model and exhibits an acceptable loss in statistical efficiency. Because of these reasons, energy based method is the author's preferred one.

According to this method, if constraints (i) and (iii) are satisfied, the square rms-value of the i -th spectral line can be estimated by taking into account the N_i WDFT samples contained inside the band B_i (Appendix A):

$$\hat{\sigma}_i^2 = \frac{2}{N^2 NNPG} \sum_{k \in B_i} |Y[k]|^2 - 2 \frac{N_i}{N} \hat{\sigma}_r^2 \quad i = 0, 1, \dots, H+S+1 \quad (7)$$

in which $NNPG = \frac{1}{N} \sum_{n=0}^{N-1} w^2[n]$ is the window normalized noise power gain [14].

Notice that when an integer number of periods of the i -th tone is observed, $N_i = 1$ and a rectangle window is employed, (7) coincides with (5). Moreover it can be shown that the estimator (7) is almost unbiased and that (Appendix B):

$$\text{var}[\hat{\sigma}_i^2] \cong \frac{4}{N} ENBW_0 \sigma_r^2 \sigma_i^2 \quad , \quad i = 0, 1, \dots, H+S+1 \quad (8)$$

where $ENBW_0 = N \sum_{n=0}^{N-1} w^4[n] / \left(\sum_{n=0}^{N-1} w^2[n] \right)^2$ represents the equivalent noise bandwidth of the squared window $w^2[\cdot]$ [15]. In particular, when a rectangle window is employed, $ENBW_0 = 1$ and (8) coincides with the corresponding *CRLB* (2). It should be pointed out that equation (8) holds for high (greater than 20) frequency domain signal-to-noise ratios [17].

Notice that, windowing increases the estimator variance of a factor equal to $ENBW_0$. However, this is usually not a problem when testing a digitizer since the estimator variance can be reduced by simply increasing the number N of analyzed samples. Conversely, the

robustness to model uncertainties, the low computational burden and the ease of use, are remarkable advantages of the estimator (7).

Notice also that, for values of N that occur in most engineering applications, the estimator (7) is almost Gaussian [16], [17].

C. Estimation of Broadband Component

When noncoherent sampling applies and constraints (i) and (ii) are satisfied, the power of the broadband noise can be estimated by means of the following relationship (Appendix A):

$$\hat{\sigma}_r^2 = \frac{1}{N_r} \frac{1}{N} \frac{1}{NNPG} \sum_{k \in B_r} |Y[k]|^2 \quad (9)$$

Observe that in the evaluation of σ_r^2 the WDFT samples related to the *DC* and the narrowband components do not have to be included. In particular, when coherent sampling applies and a rectangle window is used ($NNPG = 1$), by exploiting all of the $N/2 - (H+2)$ available samples, (9) becomes:

$$\hat{\sigma}_r^2 = \frac{2}{(N - 2H - 4)N} \left[\sum_{\substack{k=1 \\ k \neq J}}^{N/2-1} |Y[k]|^2 + \frac{1}{2} |Y[N/2]|^2 \right] \quad (10)$$

in which the power of the $N/2$ -th DFT sample is divided by 2 because it represents the total power of the digitizer output signal at the frequency $F_s/2$.

It can be shown that the estimator (9) is almost unbiased and that (Appendix B):

$$\text{var}[\hat{\sigma}_r^2] \cong \frac{1}{N_r} ENBW_0 \sigma_r^4 \quad (11)$$

Notice that (11) approaches the corresponding *CRLB* (2) when $N_r \rightarrow N/2$ and a rectangle window is used ($ENBW_0 = 1$). Moreover, when N_r is large enough, (9) is almost normally

distributed [16], [17]. Finally, if the noise is white, the value $N \cdot NNPG \cdot \hat{\sigma}_r^2$ represents an estimate of the noise floor level.

D. Estimation of overall digitizer spectral figures of merits

The estimators (7) and (9) can be used to evaluate overall digitizer figures of merits such as *SFDR*, *SNDR*, and *THD*. However, statistical analysis shows that correction factors may be needed in order to achieve accurate estimates. For instance, an almost unbiased estimator for the signal-to-random-noise ratio (*SRNR*) $\gamma_1 = \sigma_1^2 / \sigma_r^2$ is (Appendix C):

$$\hat{\gamma}_1 = \frac{N_r}{N_r + ENBW_0} \frac{\hat{\sigma}_1^2}{\hat{\sigma}_r^2} \quad (12)$$

The factor $N_r / (N_r + ENBW_0)$ is introduced in order to correct for a bias contribution induced by (11), both under coherent or noncoherent sampling conditions, and can be neglected with respect to estimation uncertainty as soon as N_r is large enough. The variance of (12) is:

$$\text{var}[\hat{\gamma}_1] \cong \frac{ENBW_0}{N_r} \gamma_1^2 \quad (13)$$

and it is due almost entirely to the variance of the broadband noise power estimator, while the contribution from the tone power estimator variance is usually negligible [6].

Observe that, when both N and N_r are great enough, (12) is almost normally distributed [16], [17].

V. CRITERIA FOR ENERGY-BASED DIGITIZER TESTING DESIGN

By applying the results described in section IV, a frequency-domain algorithm for digitizer testing can be achieved, for which all the uncertainties introduced by digital processing can be controlled by a suitable choice of algorithm parameters.

In the following, the steps involved in the design of an estimator for the square rms-values of the components of a b bit digitizer output signal will be illustrated in the case of noncoherent sampling. However, similar procedures can be employed to determine the best choice of algorithm parameters also when coherent sampling applies or when overall digitizer figures of merit are of interest.

A. Choice of the number of analyzed samples

By considering a pure sinewave as the input signal to an ideal quantizer, in order to stimulate at least once all digitizer output codes, the number of analyzed samples N has to satisfy the inequality $N \geq \pi 2^b$ [18].

A further lower bound on N is derived by setting an upper bound u_i to the normalized standard deviation $\text{std}[\hat{\sigma}_i^2]/\hat{\sigma}_i^2$ of the i -th tone power estimator. From (8) we have:

$$N \geq \frac{4}{\gamma_i} \frac{ENBW_0}{u_i^2}, \quad i = 0, 1, \dots, H+S+1 \quad (14)$$

where $\gamma_i = \sigma_i^2/\sigma_r^2$ is the signal-to-noise ratio corresponding to the i -th tone.

B. Choice of the number of WDFT samples used for the estimation of the broadband noise power

A lower bound on the number of samples inside the noise estimation band B_r can be derived by requiring that the normalized standard deviation $\text{std}[\hat{\sigma}_r^2]/\hat{\sigma}_r^2$ be less than an upper bound u_r . Hence, from (11) we have:

$$N_r \geq \frac{ENBW_0}{u_r^2}, \quad i = 0, 1, \dots, H+S+1 \quad (15)$$

Notice that (15) implies a further bound on N since the inequality $N > 2N_r$ applies.

C. Choice of the window leakage

The fraction of the i -th line power σ_i^2 that falls outside the band B_i , the so called *window leakage* L_i , depends on the shape of the window spectrum, on the number N_i of WDFT samples inside the band B_i , and on the fractional part δ_i of the recorded i -th line cycles. However, in most practical situations, all the bands B_i , $i = 1, \dots, H+S+1$ contain the same number of samples. In such a case, let L_{\max} be the maximum, with respect to δ , of L_i , $i = 1, \dots, H+S+1$. Moreover, let u_{rx} be the maximum admissible normalized bias of $\hat{\sigma}_r^2$ due to the power inside B_r from all the digitized signal tones. Then the constraint (ii) is satisfied when (Appendix D):

$$\frac{N}{2N_r} L_{\max} \gamma_x \leq u_{rx} \quad (16)$$

in which $\gamma_x = \sum_{i=1}^{H+S+1} \sigma_i^2 / \sigma_r^2$ represents the ratio between the power of all the narrow band components and the power of the broadband noise.

In particular, since for an ideal quantizer with b bits and a full-scale input sinewave we have $\gamma_x \cong 6.02 b + 1.76$ dB, (16) provides:

$$L_{\max} \leq -6.02 b - 1.76 + 10 \log_{10} u_{rx} \quad [\text{dB}] \quad (17)$$

For instance, accurate broadband noise power estimates for a 12 bit digitizer can be carried out if the window leakage related to the band B_1 is sufficiently lower than -74 dB. If samples related to window spectrum sidelobes are used to estimate the broadband noise power, this requirement is satisfied, e.g., by the 4-term minimum error energy window. Conversely, the 3-term minimum error energy window is expected to provide biased noise power estimators [6].

Observe that, since the window leakage L_{\max} decreases as the $ENBW_0$ parameter increases [19], in order to achieve estimates with minimum variance, windows with the greatest leakage that satisfies (17) should be used.

D. Choice of the number of WDFT samples used for the estimation of the narrowband component powers

In order to characterize the variability of the window leakage L_i , simulations have been carried out for different windows, by varying both δ_i and $N_i = K_i + K_{i+} + 1$, where K_i and K_{i+} represent the number of WDFT samples considered respectively on the left and on the right of the discrete spectrum peak corresponding to the i -th tone.

The window leakage $L_i = L(K_i, K_{i+}, \delta_i)$ obtained using 3- and 4-term minimum error energy windows is reported in Fig.2. These windows are considered here because of their minimum leakage property. However, similar results were achieved by considering other commonly used windows.

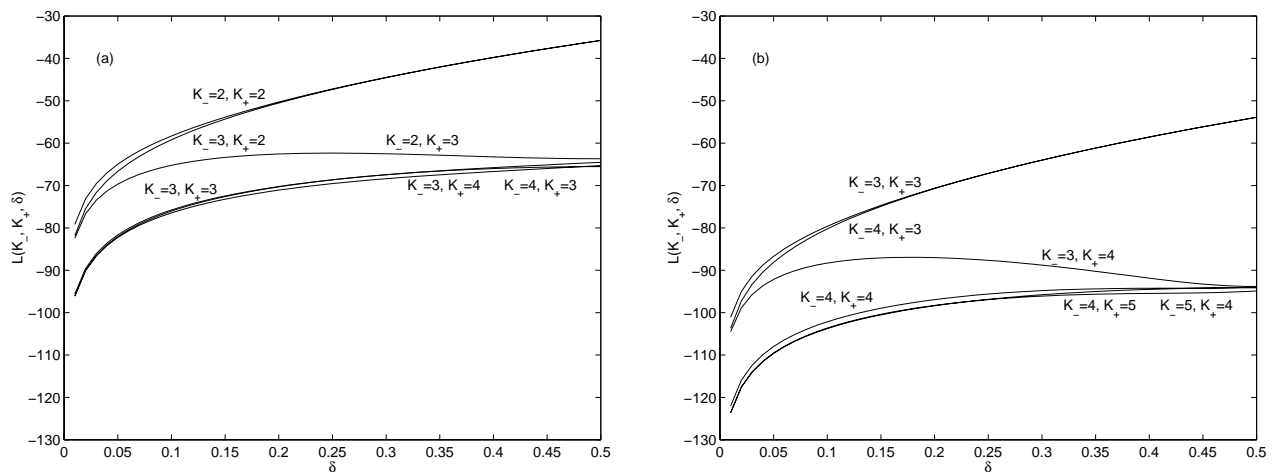


Fig. 2. Spectral leakage $L(-K_i, K_{i+}, \cdot)$ as a function of the fractional part δ_i of the recorded spectral line cycles: (a) 3-term minimum error energy window ($MLBW = 6$), (b) 4-term minimum error energy window ($MLBW = 8$).

As can be seen, WDFT samples corresponding to indexes K_i and K_{i+} greater than one half the window spectrum mainlobe bandwidth ($MLBW$), expressed in bin, provide a negligible leakage reduction. In fact, the window spectrum exhibits a very small sidelobe level. Opposite, if some WDFT samples that fall inside the window spectrum mainlobe are

excluded from processing, that is if K_i or K_{i+} are less than $MLBW/2$, the window leakage is no longer negligible, and biased estimators result.

Notice that, as K_i and K_{i+} increase, the frequency selectivity decreases and the computational effort increases. Hence optimum line power estimators are achieved when considering only all the WDFT samples that fall inside the window spectrum mainlobe.

E. Choice of the window spectrum sidelobe level

In order to estimate the i -th tone power σ_i^2 , $i = 0, 1, \dots, H+S+1$ with a negligible bias, the contribution from all other tones of the digitized signal to the power inside the set B_i must be small enough (constraint (iii)).

Consider the maximum value, normalized with respect to its peak, that the spectrum related to the j -th tone assumes inside the band B_i . This value, represented with the symbol $\overline{W}_{\max,ji}$, depends only on the envelope of the window transform and on the distance between the i -th and j -th tones. Let u_i^* be the maximum admissible value of the ratio between the power inside B_i from all tones other than the i -th one (including images) and the i -th tone power. Then constraint (iii) is satisfied when (Appendix E):

$$2 \frac{w_{CF}}{ENBW} \sum_{\substack{j=-i \\ j \neq i, -i}}^{H+S+1} \gamma_{ji} \overline{W}_{\max,ji} < u_i^* \quad (18)$$

where $w_{CF} = N \max_n(w[n]) / \left(\sum_{n=0}^{N-1} w[n] \right)$ is the crest factor of the applied window, $ENBW =$

$N \sum_{n=0}^{N-1} w^2[n] / \left(\sum_{n=0}^{N-1} w[n] \right)^2$ is its equivalent noise bandwidth [4], and $\gamma_{ji} = \sigma_j / \sigma_i$.

Notice that (18) can be satisfied by choosing a window with a sufficiently low sidelobe level [4].

F. Choice of the observation interval length

In order to provide accurate results, the proposed procedure requires the bands B_i , $i = 0, 1, \dots, H+S+1$ not to overlap (constraint (i)). If $\{F_i, i = 0, \dots, H+S+1\}$ are the frequencies (expressed in Hz) of the digitized signal tones, this occurs as soon as the length NT_S of the analyzed data record satisfies:

$$NT_S > \max_{i,j} \left\{ \frac{K_{j+} + K_{i-}}{F_j - F_i} \right\} \quad i, j = 0, \dots, H+S+1 \quad F_i < F_j \quad (19)$$

where K_{j+} and K_{i-} are the number of samples considered on the right and on the left of the discrete spectrum peaks corresponding to the i -th and j -th lines respectively.

However, (19) is not a hard to meet constraint, since observing long data records is usually not a problem in digitizer testing. Moreover, for practical applications where T_S is fixed, (19) provides an additional bound on N .

VI. EXPERIMENTAL RESULTS AND VALIDATION OF THE PROPOSED TEST PROCEDURE

A 16-bit, 20 ksample/s commercial data acquisition board has been employed to obtain experimental data for the validation of (7) through (11). A stable and highly linear sinusoidal source of frequency $F_1 = 1$ kHz and near full-scale amplitude of 9.5 V has been used to stimulate the on-board converter and to estimate the first 10 harmonics and the broadband noise power. The design of the test procedure has followed the steps described in section V.

Accordingly, the first of the two bounds on N described in subsection V.A, which guarantees in principles the excitation of all ADC output codes, provides a minimum number of samples on the order of $2 \cdot 10^5$. However, memory constraints did not allow a single-record approach. Moreover, by setting $u_i = 0.03$, $\gamma_i \geq 0.01$ for all tones, and assuming $ENBW_0 \cong 3$, as occurs for most classical windows [4], expression (14) requires N to be greater than 10^4 samples. Thus, 200 records of $N = 2^{12}$ samples each, have been collected and processed in order to satisfy both bounds simultaneously.

By setting $u_r = 0.03$, the bound (15) requires N_R to exceed 3000. It will be shown next under which conditions this bound is satisfied. By applying (17) with $u_{rx} = 0.5$, a maximum leakage about equal to -100 dB results. Thus, this constraint can be satisfied by choosing a 4-term minimum sidelobe energy window, which exhibits $MLBW = 8$ and $ENBW_0 = 2.83$ [13]. Thus, by following suggestions described in subsection V.D, K_{\downarrow} and K_{\uparrow} have been set equal to $MLBW/2 = 4$ for all tones. As described in that subsection, this choice guarantees a good compromise between estimator bias and procedure selectivity. By assuming that only $H = 10$ harmonics carry significant power, the number of samples needed to estimate their magnitudes amounts to $(K_{\downarrow}+1+K_{\uparrow}) \cdot H = (4+1+4) \cdot 10 = 90$, so that (15) is automatically satisfied when $N = 2^{12}$ samples per record are collected. Furthermore, it can be proved that (18) remains fulfilled because of the extremely low sidelobe level of the chosen window.

Finally, the parameters chosen according to previous steps provide, for each record, an observation time $NT_s \cong 0.8$ s, that largely exceeds the lower bound of $(K_{\downarrow}+K_{\uparrow})/F_1 = (4+4)/10^3 = 8$ ms provided by (19).

Obtained experimental results are presented in Tab. I. In the second column of this table the powers of output quantities estimated using (7) and (9) are reported, while in the third and fourth columns are written the corresponding experimental and theoretical standard deviations, respectively. These latter parameters have been evaluated using (8) and (11). The very good agreement between theoretical and experimental data, even for the harmonics with small magnitudes, confirms the robustness of the proposed testing procedure.

TABLE I
EXPERIMENTAL RESULTS OBTAINED USING A 16-BIT, 20 KSAMPLE/S DATA ACQUISITION BOARD

	Experimental power σ^2 [V ²]	esperimental std-deviation of σ^2 [V ²]	theoretical std-deviation of σ^2 [V ²]
noise	2.24E-08	4.4E-10	5.1E-10
fundamental	4.590E+01	3.4E-04	2.7E-05
2° harmonic	2.89E-09	2.1E-10	2.1E-10
3° harmonic	3.60E-10	7.5E-11	7.5E-11
4° harmonic	4.07E-10	7.7E-11	7.9E-11
5° harmonic	4.48E-10	7.5E-11	8.3E-11
6° harmonic	4.50E-10	8.8E-11	8.4E-11
7° harmonic	4.14E-10	8.1E-11	8.0E-11
8° harmonic	3.60E-10	8.5E-11	7.5E-11
9° harmonic	4.84E-09	7.3E-10	2.8E-10
10° harmonic	6.57E-10	5.1E-11	1.0E-10

VII. CONCLUSIONS

In this paper, performances of most common frequency-domain procedures proposed in the literature for estimating the spectral behavior of a waveform digitizer have been considered. It has been shown that, whenever possible, coherent sampling is the best choice for digitizer testing. However, when the coherency condition can not be satisfied due to digitized data or sampling circuitry characteristics, the estimation of the parameters of interest requires a suitable window sequence be applied to the digitized data prior discrete Fourier transformation.

Expressions for the variances of estimators provided by the energy based method have been presented, along with bias correction factors. The provided expressions allow both the evaluation of the algorithm accuracy and the design of the test procedure. Criteria for the selection of the optimum window sequence are also provided.

APPENDIX A

From (1) and (3) we have:

$$Y(\lambda) = CW(\lambda) + X_1(\lambda) + X_H(\lambda) + X_S(\lambda) + R(\lambda) = X(\lambda) + R(\lambda) \quad \lambda \in [0, N) \quad (\text{A.1})$$

in which $X(\cdot)$ and $R(\cdot)$ represent the WDTFT of the narrowband and broadband components of the signal (1) respectively.

In order to derive estimators for the parameters of interest, the sequence $r[\cdot] = \{r[n], n = 0, \dots, N-1\}$ is modeled as a stretch of a realization of a weakly stationary random process with flat spectrum (white noise). Moreover, constraints (i) and (iii) are assumed satisfied. Then, if σ_i and ν_i respectively represent the rms-value and the frequency of the i -th tone of digitized data, we have [13]:

$$E\left[|Y(k)|^2\right] \cong \frac{\sigma_i^2}{2} |W(k - v_i)|^2 + \sigma_r^2 N N N P G \quad \text{for } k \text{ close to } v_i \quad (\text{A.2})$$

When coherent sampling applies (that is $v_i = iJ$) and rectangle window is used, then $W(k-iJ) = N$ for $k = iJ$, and $W(k-iJ) = 0$ for $k \neq iJ$. Thus, from (A.2) the estimator (5) easily follows.

Conversely, when noncoherent sampling occurs, from (A.2) we have:

$$E\left[\sum_{k \in B_i} |Y[k]|^2\right] \cong \frac{\sigma_i^2}{2} \sum_{k \in B_i} |W(k - v_i)|^2 + \sigma_r^2 N N_i N N P G = \frac{\sigma_i^2}{2} N^2 N N P G (1 - L_i) + \sigma_r^2 N N_i N N P G \quad (\text{A.3})$$

where L_i is the fraction of the window energy that falls outside the interval B_i and depends on the fractional part δ_i of the i -th recorded tone cycles, but can be made negligible by a suitable window choice. Thus, an unbiased estimator for σ_i^2 is:

$$\hat{\sigma}_i^2 = 2 \left[\frac{1}{N^2 N N P G} \sum_{k \in B_i} |Y[k]|^2 - \frac{N_i}{N} \hat{\sigma}_r^2 \right] \frac{1}{1 - L_i} \quad i = 0, 1, \dots, H+S+1 \quad (\text{A.4})$$

Thus, the estimator (7) is directly derived from (A.4) once observed that the term L_i can be made negligible, as shown in subsection V.C. Moreover, when tones with a sufficiently high SNR are considered, even the term containing the broadband noise power estimator $\hat{\sigma}_r^2$ can be neglected.

Estimator (9) can be derived from (A.1) by observing that:

$$E\left[\sum_{k \in B_r} |Y[k]|^2\right] \cong \sigma_r^2 N N_r N N P G + \frac{N^2 N N P G}{2} \sum_{i=1}^{H+S+1} \sigma_i^2 L_{ir} \quad (\text{A.5})$$

where L_{ir} , $i = 1, \dots, H+S+1$ represents the fraction of the energy of the i -th tone that falls inside the set B_r due to spectral leakage. Such parameters depend on the fractional parts δ_i of the recorded i -th tone cycles. As shown in subsection V.C, their effect on the evaluation of

the broadband noise power can be made negligible by a suitable window choice. Under such an assumption, the estimator (9) can be easily achieved from (A.5).

APPENDIX B

In order to determine the estimator variances, expressions for auto- and cross-correlations between square modules of WDFFT samples must be known. To this purpose, from (A.1) we have:

$$\begin{aligned} \text{cov}\left[|Y[k_1]|^2, |Y[k_2]|^2\right] &= E\left[|Y[k_1]|^2 |Y[k_2]|^2\right] - E\left[|Y[k_1]|^2\right] E\left[|Y[k_2]|^2\right] = \text{cov}\left[|R[k_1]|^2, |R[k_2]|^2\right] + \\ &+ 4E\left[\text{Re}\left(Y^*[k_1]R[k_1]\right)\text{Re}\left(Y^*[k_2]R[k_2]\right)\right] + 2E\left[\text{Re}\left(Y^*[k_1]R[k_1]\right)|R[k_2]|^2\right] + 2E\left[\text{Re}\left(Y^*[k_2]R[k_2]\right)|R[k_1]|^2\right] \end{aligned} \quad (\text{B.1})$$

where the equalities $E[Y[k_1]] = E[Y[k_2]] = 0$ have been exploited and z^* represents the complex conjugate of z .

A quite simple expression for (B.1) can be achieved assuming that the random process $r[\cdot]$ has joint cumulant sequences $c_{r,k}[\cdot]$, $k = 1, \dots, 4$ that are finite, that do not depend on time shifts (*stationary condition up to order four*) and are that absolutely summable so that their spectra are bounded and uniformly continuous [20]. After some calculations we obtain:

$$\begin{aligned} \text{cov}\left[|Y[k_1]|^2, |Y[k_2]|^2\right] &= |c_{r,2}(k_1, -k_2)|^2 + |c_{r,2}(k_1, k_2)|^2 + |c_{r,4}(k_1, -k_1, k_2, -k_2)|^2 + \\ &+ 2\text{Re}\left[X^*[k_1]X[k_2]c_{r,2}(k_1, -k_2) + X^*[k_1]X^*[k_2]c_{r,2}(k_1, k_2) + X^*[k_1]c_{r,3}(k_1, k_2, -k_2) + X^*[k_2]c_{r,3}(k_2, k_1, -k_1)\right] \end{aligned} \quad (\text{B.2})$$

In practice it is of interest to determine (B.2) in the particular case when the window transform has negligible sidelobes and the random process $r[\cdot]$ has a flat spectrum up to 4-th order, which occurs when the noise samples are weakly dependent. In such a situation, it can be shown that (B.2) reduces to [13]:

$$\text{cov}\left[|Y[k_1]|^2, |Y[k_2]|^2\right] \cong |c_{r^2}(k_1, -k_2)|^2 + 2\text{Re}\left[X^*[k_1]X[k_2]c_{r^2}(k_1, -k_2)\right] \quad (\text{B.3})$$

Finally, for WDFT samples where the signal-to-noise ratio is quite high, as those closest to the i -th signal tone, we have [13]:

$$\text{cov}\left[|Y[k_1]|^2, |Y[k_2]|^2\right] \cong 2\sigma_r^2 \text{Re}\left[X^*[k_1]X[k_2]W_0(k_1 - k_2)\right] \cong \sigma_r^2 \sigma_i^2 \text{Re}\left[W^*(k_1 - v_i)W(k_2 - v_i)W_0(k_1 - k_2)\right] \quad (\text{B.4})$$

where $W_0(\cdot)$ is the transform of the squared window $w^2[\cdot]$.

Conversely, for frequencies where broadband noise dominates, we obtain [13]:

$$\text{cov}\left[|Y[k_1]|^2, |Y[k_2]|^2\right] \cong \sigma_r^4 |W_0(k_1 - k_2)|^2 \quad (\text{B.5})$$

Assume now that coherent sampling occurs for the i -th tone (that is $v_i = iJ$) and a rectangle window is applied. Since for values of N of practical interest $Y[iJ]$ exhibits a high signal-to-noise ratio and $W(0) = W_0(0) = N$, from (B.5) it follows:

$$\text{var}\left[|Y[iJ]|^2\right] = \text{cov}\left[|Y[iJ]|^2, |Y[iJ]|^2\right] \cong \sigma_r^2 \sigma_i^2 N^3 \quad (\text{B.6})$$

From (B.6) and (5), once noticed from (11) that the variability of the noise estimator $\hat{\sigma}_r^2$ can be neglected, expression (6) follows.

Analogously, since all the WDFT samples inside the band B_i exhibits a sufficiently high signal-to-noise ratio, we derive:

$$\text{var}\left[\sum_{k \in B_i} |Y[k]|^2\right] = \sum_{k_1 \in B_i} \sum_{k_2 \in B_i} \text{cov}\left[|Y[k_1]|^2, |Y[k_2]|^2\right] \cong \sigma_r^2 \sigma_i^2 \text{Re}\left[\sum_{k_1 \in B_i} \sum_{k_2 \in B_i} W^*(k_1 - v_i)W(k_2 - v_i)W_0(k_1 - k_2)\right] \quad (\text{B.7})$$

Moreover, by recalling that the band B_i contains almost all the i -th tone energy and exploiting the convolution in frequency property, we can write:

$$\begin{aligned}
\text{var} \left[\sum_{k \in B_r} |Y[k]|^2 \right] &\cong \sigma_r^2 \sigma_i^2 \text{Re} \left[\sum_{k_1=0}^{N-1} \sum_{k_2=0}^{N-1} W^*(k_1 - v_i) W(k_2 - v_i) W_0(k_1 - k_2) \right] = \\
&= \sigma_r^2 \sigma_i^2 \text{Re} \left[\sum_{k=0}^{N-1} W_0(k) \sum_{k_1=0}^{N-1} W^*(k_1 - v_i) W(k_1 - k - v_i) \right] = \sigma_r^2 \sigma_i^2 N \sum_{k=0}^{N-1} |W_0(k)|^2 = \sigma_r^2 \sigma_i^2 N^3 NNPG_0
\end{aligned} \tag{B.8}$$

where $NNPG_0 = \frac{1}{N} \sum_{n=0}^{N-1} w^4[n]$ is the normalized noise power gain of the squared window $w^2[\cdot]$.

Expression (8) now follows easily.

Opposite, for the WDFT samples inside the band B_r we have:

$$\begin{aligned}
\text{var} \left[\sum_{k \in B_r} |Y[k]|^2 \right] &= \sum_{k_1 \in B_r} \sum_{k_2 \in B_r} \text{cov} \left[|Y[k_1]|^2, |Y[k_2]|^2 \right] \cong \sigma_r^4 \sum_{k_1 \in B_r} \sum_{k_2 \in B_r} |W_0(k_1 - k_2)|^2 \cong \\
&= \sigma_r^4 \sum_{k_1 \in B_r} \sum_{k=0}^{N-1} |W_0(k)|^2 = \sigma_r^4 N_r N^2 NNPG_0
\end{aligned} \tag{B.9}$$

from which (11) can be achieved.

Various simulations were carried out in order to validate (5) through (11). Both coherent and noncoherent sampling conditions were considered, and the procedure parameters were chosen according to the criteria reported in sec. V. The good agreement between theoretical and simulation results confirms the high accuracy of the proposed expressions.

APPENDIX C

An easy and accurate expression for the statistical moments of a parameter expressed as a function $f(\cdot)$ of known random variables $\underline{\mathbf{x}}$ can be achieved by using a Taylor series expansion of $f(\cdot)$ around the mean values of $\underline{\mathbf{x}}$. In particular, if the mean and the variance of the function $\mathbf{z} = f(\mathbf{x}_1, \mathbf{x}_2)$ are of interest, we have [4]:

$$\mathbb{E}[\mathbf{z}] \cong f(\mu_1, \mu_2) + \frac{1}{2} \left[\frac{\partial^2 f}{\partial \mathbf{x}_1^2} \Big|_{\underline{\mu}} \sigma_1^2 + 2 \frac{\partial^2 f}{\partial \mathbf{x}_1 \partial \mathbf{x}_2} \Big|_{\underline{\mu}} \sigma_{12} + \frac{\partial^2 f}{\partial \mathbf{x}_2^2} \Big|_{\underline{\mu}} \sigma_2^2 \right] \quad (\text{C.1})$$

and:

$$\text{var}[\mathbf{z}] \cong \frac{\partial f}{\partial \mathbf{x}_1} \Big|_{\underline{\mu}}^2 \sigma_1^2 + 2 \frac{\partial f}{\partial \mathbf{x}_1} \frac{\partial f}{\partial \mathbf{x}_2} \Big|_{\underline{\mu}} \sigma_{12} + \frac{\partial f}{\partial \mathbf{x}_2} \Big|_{\underline{\mu}}^2 \sigma_2^2 \quad (\text{C.2})$$

in which $\mu_1 = \mathbb{E}[\mathbf{x}_1]$, $\mu_2 = \mathbb{E}[\mathbf{x}_2]$, $\sigma_1^2 = \text{var}[\mathbf{x}_1]$, $\sigma_2^2 = \text{var}[\mathbf{x}_2]$, $\sigma_{12} = \text{cov}[\mathbf{x}_1, \mathbf{x}_2]$.

Hence, approximate expressions for the mean and the variance of the ratio $\eta_1 = \hat{\sigma}_1^2 / \hat{\sigma}_r^2$ are:

$$\mathbb{E}[\eta_1] \cong \frac{\mathbb{E}[\hat{\sigma}_1^2]}{\mathbb{E}[\hat{\sigma}_r^2]} \left[1 + \frac{\text{var}[\hat{\sigma}_r^2]}{\mathbb{E}[\hat{\sigma}_r^2]^2} \right] = \gamma_1 \left[1 + \frac{ENBW_0}{N_r} \right] \quad (\text{C.3})$$

$$\text{var}[\eta_1] \cong \frac{\text{var}[\hat{\sigma}_r^2]}{\mathbb{E}[\hat{\sigma}_r^2]^2} \left[\frac{\text{var}[\hat{\sigma}_1^2]}{\text{var}[\hat{\sigma}_r^2]} + \frac{\mathbb{E}[\hat{\sigma}_1^2]^2}{\mathbb{E}[\hat{\sigma}_r^2]^2} \right] \cong \frac{ENBW_0}{N_r} \gamma_1 \left(\gamma_1 + 4 \frac{N_r}{N} \right) \cong \frac{ENBW_0}{N_r} \gamma_1^2 \quad (\text{C.4})$$

where (8) and (11) have been used and $\text{cov}[\hat{\sigma}_1^2, \hat{\sigma}_r^2]$ has been assumed negligible since only very few of the WDFT samples employed in the estimator $\hat{\sigma}_1^2$ are correlated with those used in $\hat{\sigma}_r^2$ [15].

Expressions (12) and (13) then follows from (C.3) and (C.4) respectively.

APPENDIX D

In order to derive (16), it is useful to observe that the contribution σ_{rx}^2 to the estimate of σ_r^2 due to the power inside the set B_r from all the narrow band components can be obtained from (9) and (A.5) as follows:

$$\sigma_{rx}^2 \cong \frac{N}{2N_r} \sum_{i=1}^{H+S+1} \sigma_i^2 L_{ir} \quad (D.1)$$

Since B_r is a subset of the complement of the set B_i , we have $L_i \geq L_{ir}$. Moreover, when all the bands B_i , $i = 1, \dots, H+S+1$ contain the same number of samples, we have $L_i = L(K_i, K_{i+}, \delta_i) = L(\delta_i)$. Thus:

$$\max_i L_{ir} \leq \max_i L(\delta_i) \leq \max_{0 \leq \delta < 0.5} L(\delta) = L_{\max} \quad (D.2)$$

Thus, from (D.1) and (D.2) it follows:

$$\sigma_{rx}^2 \leq \frac{N}{2N_r} L_{\max} \sum_{i=1}^{H+S+1} \sigma_i^2 \quad (D.3)$$

and:

$$\frac{\sigma_{rx}^2}{\sigma_r^2} \leq \frac{N}{2N_r} L_{\max} \gamma_x \quad (D.4)$$

in which $\gamma_x = \sum_{i=1}^{H+S+1} \sigma_i^2 / \sigma_r^2$ is the ratio between the power of all the narrow band components

and the power of the broadband noise. Finally (16) can be derived from (D.4).

APPENDIX E

Consider the WDFT of the deterministic component $x[\cdot]$ of the digitized signal (1). If σ_i , α_i , and ν_i respectively represent the rms-value, the initial phase and the frequency of the i -th tone, by taking into account also the contribution of DC offset and image tones, we have:

$$X(k) = \frac{\sigma_i}{\sqrt{2}} e^{j\alpha_i} W(k - \nu_i) + \sum_{\substack{j=-(H+S+1) \\ j \neq i}}^{H+S+1} \frac{\sigma_j}{\sqrt{2}} e^{j\alpha_j} W(k - \nu_j) \quad (E.1)$$

From (E.1) we derive:

$$\sum_{k \in B_i} |X[k]|^2 = \frac{\sigma_i^2}{2} N^2 NNPG(1-L_i) + E_i \quad (\text{E.2})$$

where:

$$\begin{aligned} E_i &\leq \sum_{k \in B_i} \left[2 \frac{\sigma_i}{\sqrt{2}} |W(k-v_i)| \left(\sum_{j \neq i} \frac{\sigma_j}{\sqrt{2}} |W(k-v_j)| \right) + \left(\sum_{j \neq i} \frac{\sigma_j}{\sqrt{2}} |W(k-v_j)| \right)^2 \right] \leq \\ &\leq W^2(0) \sigma_i^2 \sum_{k \in B_i} \left[\frac{|W(k-v_i)|}{W(0)} \left(\sum_{j \neq i} \frac{\sigma_j}{\sigma_i} \bar{W}_{\max,ji} \right) + \frac{1}{2} \left(\sum_{j \neq i} \frac{\sigma_j}{\sigma_i} \bar{W}_{\max,ji} \right)^2 \right] = \\ &= W^2(0) \sigma_i^2 \left(\sum_{j \neq i} \frac{\sigma_j}{\sigma_i} \bar{W}_{\max,ji} \right) \left[\frac{\sum_{k \in B_i} |W(k-v_i)|}{W(0)} + \frac{1}{2} \left(\sum_{j \neq i} \frac{\sigma_j}{\sigma_i} \bar{W}_{\max,ji} \right) N_i \right] \cong \\ &\cong W^2(0) \sigma_i^2 w_{CF} \left(\sum_{j \neq i} \gamma_{ji} \bar{W}_{\max,ji} \right) \end{aligned} \quad (\text{E.3})$$

in which $\bar{W}_{\max,ji} = \max_{k \in B_i} |W(k-v_j)|/W(0)$, $w_{CF} = N \max_n \{w[n]\} / \sum_n w[n]$ is the window crest-

factor, and $\gamma_{ji} = \sigma_j / \sigma_i$. The last equality in (D.3) holds since $N_i \sum_{j \neq i} \gamma_{ji} \bar{W}_{\max,ji} \ll w_{CF}$ when

the window is properly chosen.

From (E.3) we obtain an upper bound for the fraction of the power inside B_i due to tones other than the i -th one:

$$\frac{E_i}{\frac{\sigma_i^2}{2} N^2 NNPG} \leq \frac{2}{ENBW} w_{CF} \left(\sum_{j \neq i} \gamma_{ji} \bar{W}_{\max,ji} \right) \quad (\text{E.4})$$

Expression (18) now directly follows from (E.4).

REFERENCES

- [1] *Standard for Digitizing Waveform Recorders*, IEEE Std. 1057, Dec.1994.

- [2] M.Bertocco, C.Narduzzi, P.Paglierani, D.Petri, "A noise model for digitized data", *IEEE Trans. Instrum. Meas.*, vol. 49, no. 1, pp. 83-86, Feb. 2000.
- [3] S.L.Marple, *Digital Spectral Analysis with Applications*, Englewood Cliffs, N.J.: Prentice Hall, 1987.
- [4] F.J. Harris, "On the Use of Windows for Harmonic Analysis with the Discrete Fourier Transform.," *Proc. IEEE*, vol. 66, pp. 51-83, Jan. 1978.
- [5] S.M. Kay, *Fundamentals of Statistical Signal Processing*, Prentice-Hall, 1998.
- [6] M.Bertocco, C.Narduzzi, P.Paglierani, D.Petri, "Accuracy Performances of ADC Parameter Estimators", *Proc. IEEE Instrum. Meas. Tech.. Conf.*, Ottawa, Canada, 19-21 Mag. 1997, pp. 985-988.
- [7] P.Carbone, D.Petri, "Accurate Equivalent-time Sampling", *Proc. 4-th Workshop on ADC Modelling and Testing*, Bordeaux, France, 9-10 Sept. 1999, pp. 119-122.
- [8] M.Bertocco, P.Carbone, F. Zanin, "Statistical Analysis of Frequency-domain Estimation Methods for Multiple Tone Signal Parameters", *Proc. Intern. Workshop on Advanced Mathematical Modelling in Electrical and Electronic Measurement*, Como, Italy, 6-8 July 1994, pp. 241-261.
- [9] G.Andria, M.Savino, A. Trotta, "FFT-based Algorithms Oriented to Measurements on Multifrequency Signals", *Measurement*, vol.12, pp. 25-42, Dec. 1993.
- [10] I.Kollar, "Evaluation of Sinewave Tests of ADC's from Windowed Data", *Proc. 4-th Intern. Workshop on ADC Modelling and Testing*, Bordeaux, France, 9-10 Sept. 1999, pp. 64-68.
- [11] P.Carbone, E.Nunzi, D.Petri, "Frequency-domain based Least-squares Estimation of Multifrequency Signal Parameters", *IEEE Trans. Instrum. Meas.*, vol.IM-49, no.2, Apr. 2000, pp.337-340
- [12] D.C. Rife, R.R. Boorstyn "Multiple Tone Parameter Estimation from Discrete Time Observations", *Bell Syst. Tech. Jour.*, vol. 55, no. 9, pp. 1389-1410, Nov. 1976.
- [13] L.Benetazzo, C.Narduzzi, C.Offelli, D.Petri, "A/D Converter Performance Analysis by a Frequency Domain Approach", *IEEE Trans. Instrum. Meas.*, vol. 41, no. 6, pp. 834-839, Dec. 1992.
- [14] O.M. Solomon, Jr., "The Use of DFT Windows in Signal-to-Noise Ratio and Harmonic Distortion Computations," *IEEE Trans. Instrum. Meas.*, vol. 44, no. 2, pp. 194-199, Apr. 1994.
- [15] C.Offelli, D.Petri, "Weighting Effect on the Discrete Time Fourier Transform of Noisy Signals", *IEEE Trans. Instrum. Meas.*, vol.IM-40, no.6, pp.972-981, Dic. 1991.
- [16] J. Schoukens and J. Renneboog, "Modelling the Noise Influence on the Fourier Coefficients After a Discrete Fourier Transform", *IEEE Trans. Instrum. Meas.*, vol. 35, no. 3, pp. 278-286, Sept. 1986.
- [17] C.Offelli, D.Petri, "The Influence of Windowing on the Accuracy of Multifrequency Signal Parameter Estimation", *IEEE Trans. Instrum. Meas.*, vol.IM-41, no.2, pp.256-261, Apr. 1992.
- [18] European Project DYNAD, "Methods and draft standards for the DYNamic characterisation and testing of Analogue to Digital converters", published in internet at <http://www.fe.upt.pt/hsm/dynad>.
- [19] D. Slepian, "Prolate Spheroidal Wave Functions, Fourier Analysis and Uncertainty – V: The Discrete Case," *Bell Syst. Tech. Journ.*, vol.57, pp.1371-1430, May-June 1978.
- [20] D.R. Brillinger, P.R.Krishnaiah, *Time Series in the Frequency-Domain*, Amsterdam: North Holland, 1983, pp.21-38.